Rheol Acta (2009) 48:543–550
DOI 10.1007/s00397-009-0350-3

ORIGINAL CONTRIBUTION

An experimental evaluation of the behaviour of mono and polydisperse polystyrenes in Cross-Slot flow

D. G. Hassell · M. R. Mackley

Received: 22 July 2008 / Accepted: 11 February 2009 / Published online: 13 March 2009

Abstract The behaviour of a number of mono and polydisperse polystyrenes are probed experimentally in complex extensional flow within a Cross-Slot geometry using flow-induced birefringence. Polystyrenes with similar molecular weight (M_w) and increasing polydispersity (PD) illustrated the effect of PD on the principal stress difference (PSD) pattern in extensional flow. Monodisperse materials exhibited only slight asymmetry at moderate flowrates, although increased asymmetry and cusping was observed at high flowrates. The response of monodisperse materials of different M_w at various flowrates is presented and characterised by Weissenberg numbers for both chain stretch and orientation using a theory for linear entangled polymers. The comparison of stress profiles against Weissenberg number for each process is used to determine whether the PSD pattern observed is independent of M_w and elucidate which relaxation mechanism is dominant in the flow regimes probed. For monodisperse materials, at equivalent chain orientation Weissenberg number ($We_{\tau d}$), different molecular weight materials were seen to exhibit similar steady state PSD patterns independent of $We_{\tau R}$ (chain stretch We). Whilst no obvious critical Weissenberg number (We) was found for the onset of increased asymmetry and cusping, it was found to occur in the "orientating flow without chain stretch" regime.

Keywords Monodisperse polystyrene · Elongational flow · Birefringence

D. G. Hassell · M. R. Mackley (✉)
Department of Chemical Engineering,
University of Cambridge, Pembroke Street,
Cambridge, CB2 3RA, UK
e-mail: mrm5@cam.ac.uk

Present Address:
D. G. Hassell
Department of Chemical Engineering,
University of Nottingham Malaysia Campus,
Jalan Broga, 43500 Semenyih, Selangor D.E., Malaysia

Introduction

Monodisperse materials, with their precisely controlled molecular architecture, are useful model systems to provide benchmark experiments for comparison with theory. Due to the limited sample sizes available, there are few studies using these model materials in complex flows, and those available have mainly been carried out in predominantly simple shear flows (see for instance, Collis and Mackley 2005). Materials behave differently in simple shear and pure shear flows and large strain extensional flow deformations are capable of probing rheological aspects of polymer melt behaviour that are not necessarily revealed in simple shear flow. A range of rheometers have been designed for study in extensional deformation (see for instance Taylor 1934; Frank and Mackley 1976; Crowley et al. 1976; Scrivener et al. 1979; Sridhar et al. 1991; Meissner and Hostettler 1994) and in this work a Cross-Slot geometry (see for instance Verbeeten 2001; Soulages et al. 2008a, b, Coventry and Mackley 2008) is used to create a region of high extensional deformation along the inlet–outlet symmetry plane. The behaviour of a number of mono and polydisperse polystyrenes are probed using flow-induced birefringence. Polystyrenes with similar molecular weight (M_w) and increasing polydispersity (PD) illustrate the effect of PD on the principal stress difference

(PSD) pattern in extensional flow. The response of monodisperse materials of different M_w at various flowrates is captured and characterised by Weissenberg numbers for both chain stretch and orientation using a theory for linear entangled polymers (Likhtman and McLeish 2002). The comparison of stress profiles against Weissenberg number for each process is used to determine whether the PSD pattern observed is independent of M_w and elucidate which relaxation mechanism is dominant in the flow regimes probed.

Materials

The polymers used were all polystyrenes, and since they share a common chemical structure, the differences between them can be linked to their differing molecular weight distributions. Four monodisperse polystyrenes and two polydisperse materials were used and the properties of these are summarised in Table 1. The monodisperse materials have a polydispersity between 1.1 and 1.2 and increasing molecular weights (M_w) ranging from 118–488 kg/mol. The polydisperse materials have an M_w roughly similar to each other and one of the monodisperse materials (DOW1570, $M_w \approx 305$ kg/mol) but increasing polydispersity (PD) from 2–4.6.

Processing experiments

A Cambridge Multi-Pass Rheometer (MPR) (Mackley et al. 1995) was used for the processing experiments and its application with an optical configuration has been previously described by a number of authors (see for instance, Collis and Mackley 2005). The MPR is a dual piston capillary-type rheometer designed for small quantities of material (~10 g of polymer) and consists of three sections. The top and bottom sections contain reservoirs for the polymer material, servo hydraulically driven pistons and pressure/temperature transducers. The midsection enables simultaneous pressure and optical measurements to be made and resembles a cube with holes in all six faces. The vertical faces accept a pair of stainless steel die inserts in one direction and a pair of 15-mm depth stress-free quartz windows in the other, while polymer flows through the top and bottom holes. All three sections are surrounded by heating channels and insulation. While the heating jackets ensure a constant temperature around the three sections, heat losses are likely to occur through the quartz windows. These have not been quantified, but are expected to be small (from Kalpokaite-Dichkuvene and Stravinskas 2006, the heat-conductivity coefficients of steel and quartz are given as 42 and 1.3 W/(mK) respectively). The inserts used for the Cross-Slot geometry utilised slave pistons which used a pressurised nitrogen system to facilitate multi-pass operation. The system was developed by Coventry (2006) and was reported by Coventry and Mackley (2008). During operation, the two MPR pistons are moved towards one another at a controlled rate, pushing material in to the insert through the top and bottom channels and out through two horizontal side channels. Slave pistons in these horizontal channels maintain the material within the MPR and the subsequent retraction of the pistons to their original position allows the pressurised nitrogen to force the material back through the Cross-Slot and into the top and bottom reservoirs. A schematic of the MPR and the geometry of the Cross-Slot are shown in Fig 1.

This geometry has been used in previous work (Coventry and Mackley 2008; Hassell and Mackley 2008; Hassell et al. 2008) and is 10-mm deep. While the aspect ratio is around 7, equating approximately to two-dimensional flow (Wales 1976), three-dimensional effects are possible. Previous work has concluded that this three-dimensional effect may not have a great impact on the observed birefringence (Clemeur et al. 2004) and that these effects are enhanced by branching (Hertel et al. 2008). In all cases the assumption of two-dimensional flow is only approximate and the results reported here are expected to deviate quantitatively slightly from the ideal two-dimensional case.

Stress-induced birefringence was used to observe the principal stress difference during flow. Monochromatic polarised light with a wavelength of 514 nm was passed through the midsection and orthogonal analyzer before being captured using a digital video camera. Quarter wave plates were used to eliminate the isoclinic extinction bands and leave only the stress-related isochromatic fringes. A telecentric lens was used, and when coupled with the CCD camera (resolution 1,280 × 960 pixels) gave a maximum resolution of approximately 4.5×10^{-3} mm per pixel (220 pixels per mil-

Table 1 Table of material molecular weights and polydispersity determined using gel permeation chromatography (GPC) with THF as the solvent

Label	M_w (g/mol)	M_n (g/mol)	M_w/M_n
DOW1568	118,300	105,000	1.128
DOW1569	207,900	181,400	1.146
DOW1570	304,800	260,800	1.169
DOW1571	488,500	410.149	1.191
PS648	333,300	162,800	2.05
PS4040915	338,000	73,500	4.6

All measurements were undertaken with the same calibration

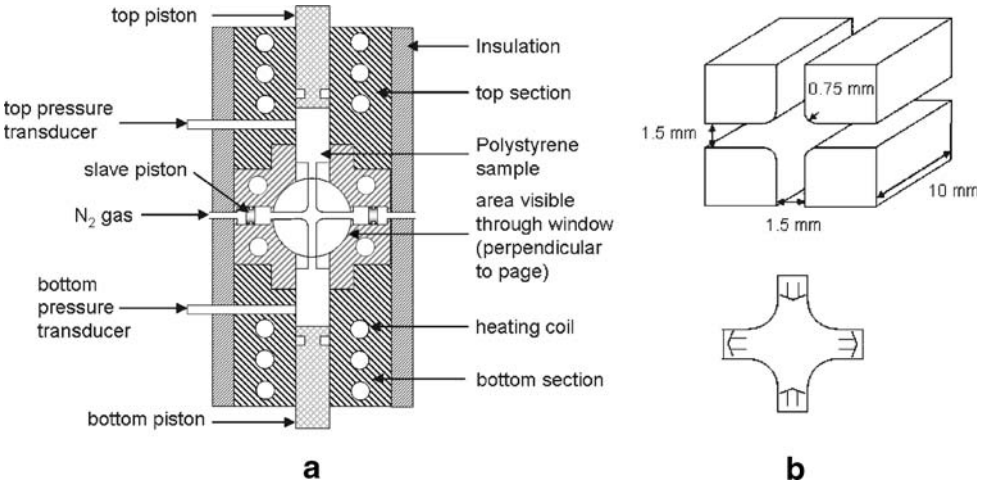

Fig. 1 **a** Schematic outlining the MPR and **b** the dimensions and flow direction for the Cross-Slot geometry

limeter). Optically, it was only possible to observe half fringes (either white or black) of order 2 pixels width, which gave a fringe resolution of order 2×10^{-2} mm. It is currently not possible using the set-up to resolve stress fringes with greater concentration than this.

The central extension rate in the Cross-Slot was estimated from the flow geometry and the relationship between the maximum extension rate and the piston speed was defined as

$$\dot{\varepsilon}_{\max} = AV_p \tag{1}$$

where A is a constant defined by the geometry with units mm^{-1}. Previous work has reported A to be 8.6 (Hassell et al. 2008) and this value is also used here.

The Weissenberg number can be used to characterise the level of deformation experienced by the polymer and is given by

$$We = \dot{\varepsilon}_{\max}\tau \tag{2}$$

where τ is a characteristic relaxation time. For monodisperse materials this relaxation time can be either the chain stretch relaxation time, τ_R (also referred to as the Rouse time), or the orientation relaxation time, τ_d (also referred to as the reptation time). This provides two Weissenberg numbers based on either chain stretch ($We_{\tau\text{R}}$) or orientation ($We_{\tau\text{d}}$).

Results and discussion

Figure 2 shows steady state principal stress difference (PSD) profiles for one monodisperse and two polydisperse materials at the same processing conditions. While there is a slight increase in M_w ($M_\text{w} \approx$ 300 kg/mol), the main difference in the materials is the increasing polydispersity (PD) from ≈1.2 to 4.6. The PSD level in the shear flow region at the inlet to the Cross-Slot is similar for all three materials, indicating that in this type of flow there is no obvious difference in material behaviour. However, along the inlet–outlet centreline the asymmetry and level of centreline "cusping" is seen to increase with increasing PD.

Materials with increasing PD have a greater proportion of high molecular weight chains, as represented by the differences in M_n and M_w shown in Table 1. These chains have longer relaxation times, illustrated in Fig. 3, which shows the contribution of each mode

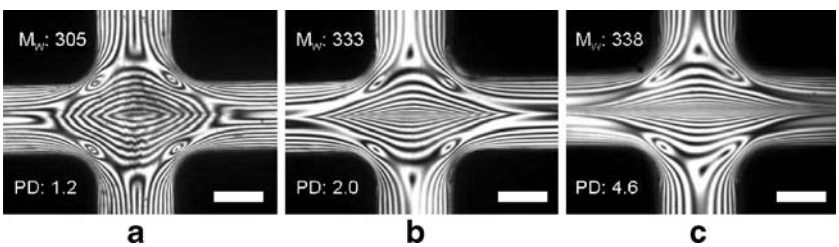

Fig. 2 Steady state birefringence profiles for **a** monodisperse PS1570, **b** polydisperse PS648 and **c** polydisperse PS4040915. In all three cases the temperature is 180°C, flowrate per inlet is 3.46 $\text{mm}^3\ \text{s}^{-1}$ and extension rate is ≈0.38 s^{-1}. In each image the *white bar* represents 1 mm in length, and material flows into the Cross-Slot through the vertical channels and out through the horizontal ones

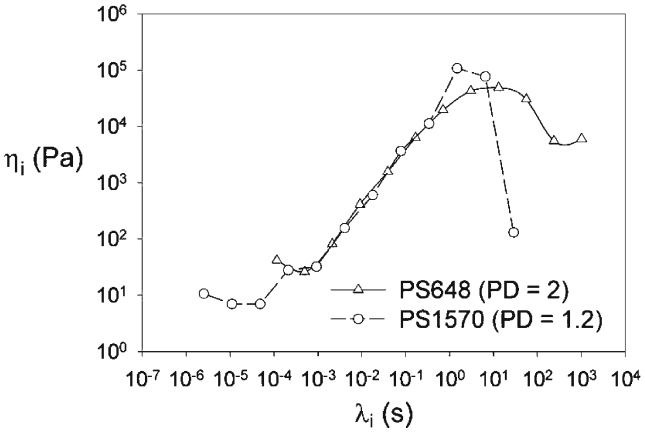

Fig. 3 Plot of zero shear viscosity of each relaxation mode, $\eta_i = G_i \times \lambda_i$, as a function of relaxation time, λ, using Maxwell modes fitted to oscillatory rheology. The rheology for PS1570 was provided by John Embery at Leeds University and for PS648 by Rudy Valette at CEMEF

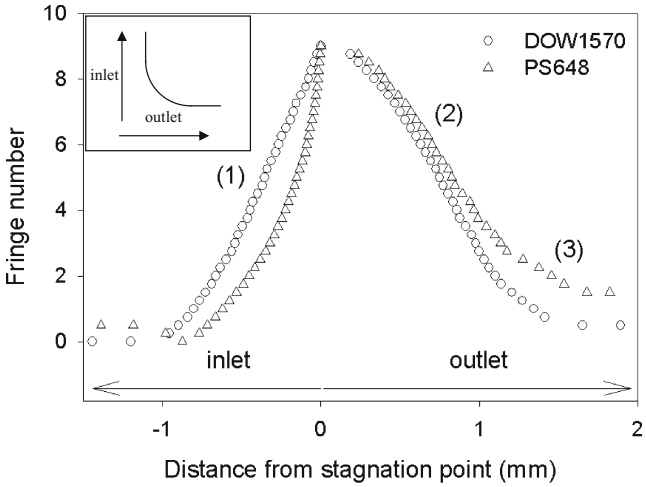

Fig. 4 The principal stress difference profile along the inlet outlet centreline for DOW1570 (*circle*) and PS648 (*triangle*) at a temperature of 180°C, flowrate per inlet of 3.46 mm^3 s^{-1} and extension rate of ≈0.38 s^{-1}. The *y* axis represents the contour number of the fringe at any given location with reference to that at zero PSD (and hence zero light retardation)

to the zero shear viscosity for two of the materials; the monodisperse material (PS1570) and the first polydisperse material (PS648). In this figure, the increasing contribution of the longer relaxation modes to the zero shear viscosity is clearly seen for PS648, and hence this material exhibits an increased "elastic behaviour" during flow. In the region upstream of the Cross-Slot, these longer relaxation modes have a limited affect on the PSD observed due to the low strains present there. As the material moves closer to the stagnation point, the residence time for the material increases (see for instance, Crowley et al. 1976) and this results in greater strain. At these higher strains, the higher molecular weight materials become increasingly stretched within the flow, and on exiting the stagnation region these molecules take longer to relax. This results in the "cusping" shown in Fig. 2b, c, and illustrates elegantly the effect that the long molecular weight chains, present in increasing numbers as PD increases, have in flow which is subjected to high strain.

This is further shown in Fig. 4, illustrating the fringe number against position along the inlet–outlet centre line for the images shown in Fig. 2a, b. As the materials flow along the inlet centreline towards the stagnation point, region 1 in the graph, the PSD response is different for each material. The increase in stress, with reference to proximity to the stagnation point, is linear for the monodisperse material and non-linear for the polydisperse material. Once the materials pass through the stagnation point and begin to move along the outlet centreline, region 2 in the graph, the initial decay in PSD with position is similar for both materials. As the distance away from the stagnation point along the outlet centre line continues to increase, region 3 in the graph, the PSD of the monodisperse material falls to zero while the PSD decay in the polydisperse material more closely resembles exponential decay. The behaviour in region 1 and 3 are caused by the increasing influence of the past deformation on the current PSD of the material due to the increased "memory" of the high M_w chains. The longer relaxation modes illustrated in Fig. 3 for the polydisperse material have an increased effect on the observed stress pattern as the level of strain increases. The similarity in the initial decay after the stagnation point (in region 2) is the result of the quicker relaxation of the lower M_w chains present in both materials. This can be seen by the almost identical contribution to the zero shear viscosity in Fig. 3 of the modes in the range of λ_i from 10^{-3} s to above 10^{-1} s for both materials.

The effect of increasing M_w for monodisperse materials is shown in Fig. 5, highlighting the steady state PSD profiles for two monodisperse materials (PS1569, $M_w \approx$ 208 kg/mol, and PS1570, $M_w \approx 305$ kg/mol) at the same processing conditions. While there are more fringes for the higher M_w case, there is no obvious increase in the level of asymmetry for the two materials. Like the work of Collis and Mackley (2005) in the contraction expansion (CE) slit flow, these results provide a useful set of validation data for both theory and software aimed at predicting the behaviour of these polymeric materials in the Cross-Slot.

A sequence of steady state PSD images of DOW1569 ($M_w \approx 208$ kg/mol) at increasing flowrates is given in

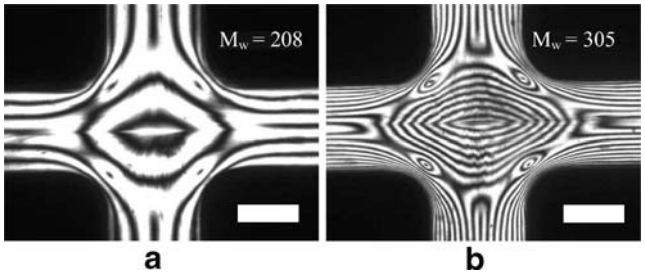

Fig. 5 Steady state birefringence profiles for **a** monodisperse PS1569 ($M_w \approx 208$ kg/mol) and **b** monodisperse PS1570 ($M_w \approx 305$ kg/mol). In both cases the temperature is 180°C, flowrate per inlet is 3.46 mm^3 s^{-1} and extension rate is ≈0.38 s^{-1}. In each image the *white bar* represents 1 mm in length and materials flows into the Cross-Slot through the vertical channels and out through the horizontal ones

Fig. 6. For the lowest flowrate, Fig. 6a, the pattern is nearly Newtonian (see for instance Coventry 2006), with only a slight asymmetry close to the stagnation point. As the flowrate increases, Fig. 6b, c, the level of PSD increases, and only a slight change in the qualitative pattern is observed. At the highest flowrate, Fig. 6d, high levels of PSD and a large asymmetry are seen between the inlet and outlet with centreline cusping similar to the polydisperse materials.

The flow of monodisperse materials has been categorised by Collis et al. (2005) into three regimes exhibiting (1) linear response ($We_{\tau d} < 1$, $We_{\tau R} < 1$),

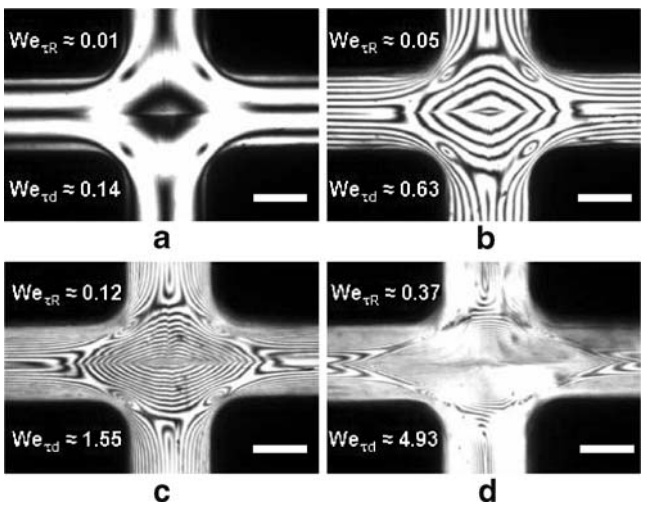

Fig. 6 Steady state birefringence images of DOW1569 (M_w 208 kg/mol) at 180°C for extension rates of **a** ≈0.17 s^{-1}, **b** ≈0.77 s^{-1}, **c** ≈1.89 s^{-1} and **d** ≈6.02 s^{-1}. The corresponding Weissenberg numbers based on both the Rouse and reptation times are given with each of the images. In each image the *white bar* represents 1 mm in length, and material flows into the Cross-Slot through the vertical channels and out through the horizontal ones

(2) orientating flow without chain stretch ($We_{\tau d} > 1$, $We_{\tau R} < 1$) and (3) orientating flow with chain stretch ($We_{\tau d} > 1$, $We_{\tau R} > 1$). To ascertain whether the shift in PSD pattern seen in Fig. 6d was the result of a critical Weissenberg number, the orientation (τ_d) and chain stretch (τ_R) relaxation times for each polymer were fitted using a theory for linear entangled polymers (Likhtman and McLeish 2002). The molecular weight is used to obtain a value of Z from the theory, where $Z = M_w/M_e$ (weight averaged molecular weight divided by the entanglement molecular weight) which is then used to obtain the relaxation times;

$$\tau_R = \tau_e Z^2 \tag{3}$$

$$\tau_D = 3\tau_e Z^3 \left(1 - \frac{2C_1}{\sqrt{Z}} + \frac{C_2}{Z} + \frac{C_3}{Z^{3/2}}\right) \tag{4}$$

For these equations, the values $C_1 = 1.69$, $C_2 = 4.17$ and $C_3 = -1.55$ were used. The relaxation times used are presented in Table 2 and the Weissenberg numbers included in Fig. 6 illustrate that the cusping is seen within regime 2 ($We_{\tau d} > 1$, $We_{\tau R} < 1$) and hence seemingly a result of orientation and not chain stretch.

To evaluate the effect of the orientation and stretch relaxation times, it is useful to vary one Weissenberg number while maintaining the other at a constant value. For monodisperse polystyrenes, the ratio of the two relaxation times is a function of molecular weight. By varying the materials used, it is possible to create a set of processing conditions where *We* for one relaxation time is almost constant while varying the other.

Figure 7 shows the steady state PSD pattern for each of the four materials at $We_{\tau R} \approx 0.06$, with $We_{\tau d}$ ranging from 0.26–2.6. While it can be seen that an increase in $We_{\tau d}$ from Fig. 7a–d leads to an increasing level of PSD and Fig. 7d has increased asymmetry, there is no obvious progressive development of the cusping and no sharp transition at $We_{\tau R} \geq 1$.

Figure 8 shows the four monodisperse materials with a constant $We_{\tau d} \approx 2.5$, but with $We_{\tau d}$ ranging from 0.54–0.058. While it is not possible to compare the level of

Table 2 Table of orientation and chain stretch relaxation times for the monodisperse materials at their processing conditions

Label	M_w (g/mol)	Temperature (°C)	τ_d (s)	τ_R (s)
DOW1568	118,300	150	2.83	0.627
		180	0.077	0.017
DOW1569	207,900	180	0.82	0.0621
DOW1570	304,800	180	3.08	0.132
DOW1571	488,500	180	15.2	0.336

This was done using Reptate, software developed by Likhtman and Ramirez at the University of Leeds

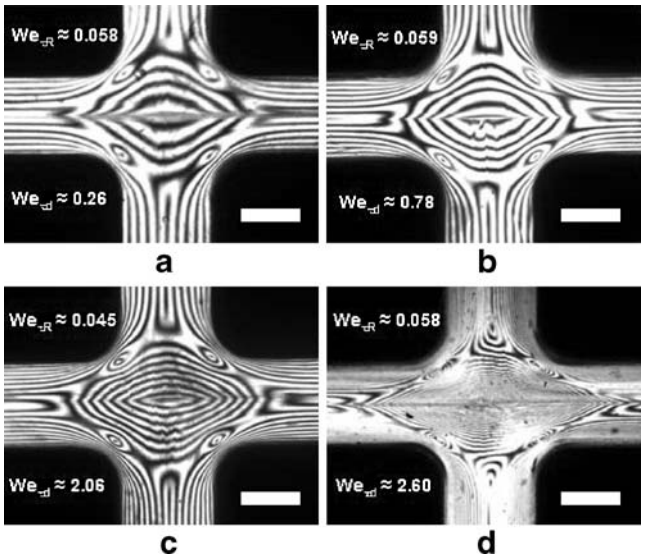

Fig. 7 Steady state birefringence images at equivalent Rouse averaged Weissenberg number for **a** DOW1568 (M_w 118 kg/mol) at 150°C, **b** DOW1569 (M_w 208 kg/mol) at 180°C, **c** DOW1570 (M_w 307 kg/mol) at 180°C and **d** DOW1571 (M_w 488 kg/mol) at 180°C. The lower processing temperature for DOW1568 was used to attain higher Weissenberg numbers for this material, which are given in the images. In each image the *white bar* represents 1 mm in length, and material flows into the Cross-Slot through the vertical channels and out through the horizontal ones

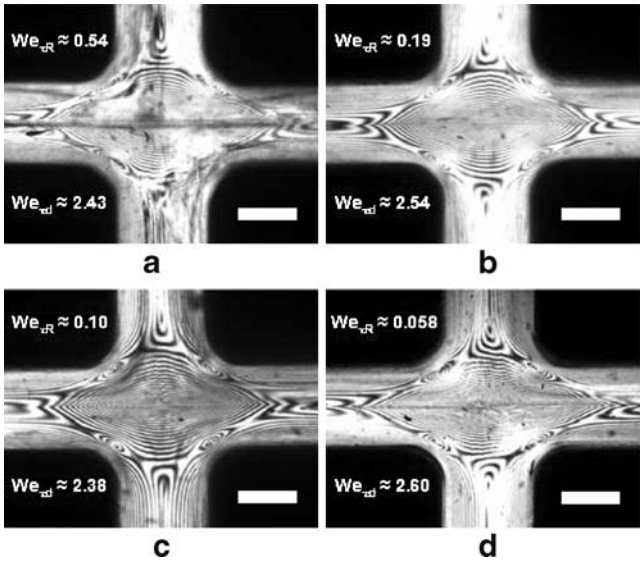

Fig. 8 Steady state birefringence images at equivalent reptation averaged Weissenberg number for **a** DOW1568 (M_w 118 kg/mol) at 150°C, **b** DOW1569 (M_w 208 kg/mol) at 180°C, **c** DOW1570 (M_w 307 kg/mol) at 180°C and **d** DOW1571 (M_w 488 kg/mol) at 180°C. The lower processing temperature for DOW1568 was used to attain higher Weissenberg numbers for this material, which are given in the images. In each image the *white bar* represents 1 mm in length, and material flows into the Cross-Slot through the vertical channels and out through the horizontal ones

PSD due to the high number of fringes, a similarity in the patterns is observed. Thus, within regime 2 (orientating flow without chain stretch), it is the orientation which defines the observed PSD pattern in these monodisperse materials. This is perhaps unsurprisingly given that the molecules are predicted by theory to be subjected to no chain stretch within this region with only orientation present. Hence, different materials processed at different temperatures show similar stress patterns when their orientation Weissenberg numbers are matched within this flow.

While it was not possible to probe deeply into the orientating flow with chain stretch regime, it was possible to reach values of $We_{\tau R} \approx 1$ by lowering the temperature for DOW1568. An example of this is shown in Fig. 9, which compares the steady state PSD pattern for the two lowest M_w materials, ($M_w \approx 118$ kg/mol and ≈ 208 kg/mol) at roughly similar $We_{\tau d}$. In this case $We_{\tau R}$ is in regime 3 for Fig. 9a and regime 2 for Fig. 9b. It would be presumed that the affects of chain stretch close to the stagnation point would lead to enhanced "cusping" and a change in the PSD pattern from that previously seen. Comparison between Fig. 9a and b shows this not to be the case, with no obvious difference in the patterns. Figure 9c shows a montage of the two areas of Fig. 9a, b highlighted in the boxes, and further illustrates the similarities between the two. The conclusion drawn from this is that there is noticeable effect on the PSD of an increase in chain stretch close to the stagnation point, with orientation dominating the overall flow.

It is important to note that it is impossible to pick out the features along the outlet centreline close to the stagnation point for Fig. 9 due to the image resolution outlined in the "Processing experiments" section. Chain stretch is expected to occur over a small area close to the stagnation region and it is possible therefore that any change in the pattern is not visible in these images. Another important consideration is the validity of the stress optical rule at these high stresses. Work for polystyrene melts (Venerus et al. 1999) found a deviation of the stress optic rule above roughly 1 MPa in uniaxial extensional flow, although this value decreases for increasing polydispersity and decreasing Weissenberg number (Luap et al. 2006). With a stress optical coefficient of order -4.3×10^{-9} Pa^{-1} for DOW1569 (Coventry 2006), it is possible that this limit is exceeded in the flows of Figs. 8 and 9, so caution should be made when interpreting these results. However, the results in Figs. 7, 8 and 9 do indicate that within the conditions probed, the PSD pattern is determined by the orientation relaxation time. Different M_w materials

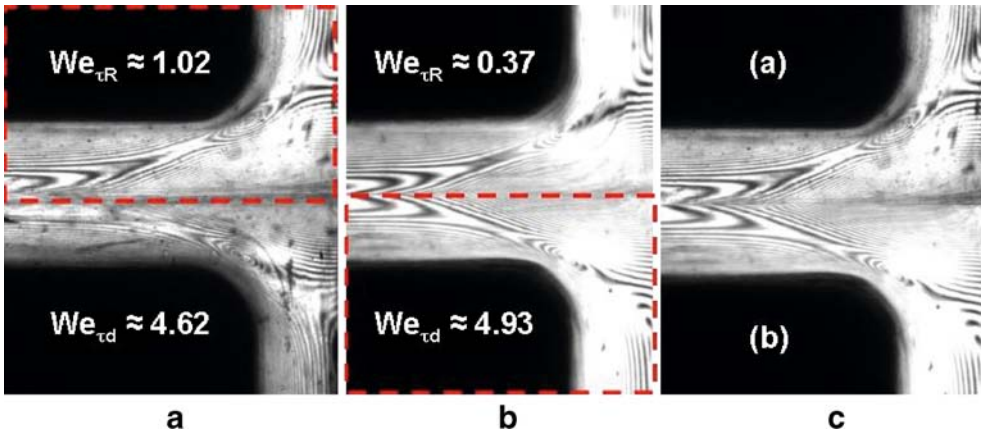

Fig. 9 Steady state birefringence images at equivalent reptation averaged Weissenberg number for **a** DOW1569 (M_w 208 kg/mol) at 180°C and **b** DOW1568 (M_w 118 kg/mol) at 150°C. The lower processing temperature for DOW1568 was used to attain higher Rouse averaged Weissenberg numbers, which are given in the images. The areas highlighted in the *doted boxes* from **a** and **b** are combined to compare the two PSD patterns and is given in (**c**). Material flows into the Cross-Slot through the vertical channels and out through the horizontal ones

exhibit similar stress behaviour at similar $We_{\tau d}$, and it should be possible to predict the PSD pattern purely based on this relaxation time, independent of M_w.

Conclusions

The behaviour of mono and polydisperse polystyrenes in complex extensional flow was captured using flow-induced birefringence. For similar processing conditions and equivalent molecular weight (M_w), an increase in polydispersity (PD) led to an increase in asymmetry and centreline "cusping" in the principal stress difference (PSD). For monodisperse materials, the PSD pattern was found to develop from slight to high asymmetry and the formation of centreline "cusping" with an increase from moderate to high flowrates. A theory for linear entangled polymers (Likhtman and McLeish 2002) was used to obtain Weissenberg numbers for both orientation ($We_{\tau d}$) and chain stretch ($We_{\tau R}$). These were used to evaluate the effect of these two relaxation times on the observed PSD, and "cusping" was found to occur in the orientating flow without chain stretch ($We_{\tau d} > 1$, $We_{\tau R} < 1$) regime. For the conditions interrogated, orientation was found to determine the PSD pattern and at equivalent $We_{\tau d}$, all four materials were seen to exhibit similar steady state PSD patterns independent of $We_{\tau R}$.

Acknowledgements Both authors would like to acknowledge DOW for materials, Lian Hutchings for the GPC data and Simon Butler for technical assistance. This work was funded through the Microscale Polymer Processing Project, EPSRC Contract No. GR/T11807/01.

References

Clemeur N, Rutgers RPG, Debbaut B (2004) Numerical evaluation of three dimensional effects in planar flow birefringence. J Non-Newton Fluid Mech 123:105–120

Collis MW, Mackley MR (2005) The melt processing of monodisperse and polydisperse polystyrene melts within a slit entry and exit flow. J Non-Newton Fluid Mech 128(1):29–41

Collis MW, Lele AK, Mackley MR, Graham RS, Groves DJ, Likhtman AE, Nicholson TM, Harlen OG, McLeish TCB, Hutchings L, Fernyhough CM, Young RN (2005) Constriction flows of monodisperse linear entangled polymers: multiscale modelling and flow visualization. J Rheol 49 (2):501

Coventry KD (2006) Cross-Slot rheology of polymers. PhD thesis, Department of Chemical Engineering, University of Cambridge

Coventry KD, Mackley MR (2008) Cross-slot extensional flow of polymer melts using a multi-pass rheometer. J Rheol 52:401–415

Crowley DG, Frank FC, Mackley MR, Stephenson RG (1976) Localised flow birefringence of polyethylene oxide solutions in a four roll mill. J Polym Sci 14:1111–1119

Frank FC, Mackley MR (1976) Localized flow birefringence of polyethylene oxide solutions in a two roll mill. J Polym Sci A2 14:1121–1131

Hassell DG, Mackley MR (2008) Localised flow induced crystallisation of a polyethyelene melt. Rheol Acta 47:435–446. doi:10.1007/s00397-008-0263-6

Hassell DG, Auhl D, McLeish TCB, Mackley MR (2008) The effect of viscoelasticity on stress fields within polyethylene melt flow for a Cross-Slot and contraction-expansion slit geometry. Rheol Acta 47:821–834. doi:10.1007/s00397-008-0261-8

Hertel D, Vallette R, Münstedt H (2008) Three-dimensional entrance flow of a low-density polyethylene (LDPE) and a

linear low-density polyethylene (LLDPE) into a slit die. J Non-Newton Fluid Mech 153:82–94
Kalpokaite-Dichkuvene R, Stravinskas G (2006) Behaviour of a fuel oil droplet on a hot surface. J Eng Phys Thermophys 79(1):10–17
Likhtman AE, McLeish TCB (2002) Quantitative theory for linear dynamics of linear entangled polymers. Macromolecules 35:6332–6343
Luap C, Karlina M, Schweizer T, Venerus DC (2006) Limit of validity of the stress-optical rule from polystyrene melts: influence of polydispersity. J Non-Newton Fluid Mech 138(2–3):197–203
Mackley MR, Marshall RTJ, Smeulders JBAF (1995) The multipass rheometer. J Rheol 39(4):1293–1309
Meissner J, Hostettler J (1994) A new elongational rheometer for polymer melts and other highly viscoelastic liquids. Rheol Acta (33(1):1–21
Scrivener O, Berner C, Cressely R, Hocquart R, Sellin R, Vlaches NS (1979) Dynamical behaviour of drag-reducing polymer solutions. J Non-Newton Fluid Mech 5:475–495
Sridhar T, Tirtaatmadja V, Nguyan DA, Gupta RK (1991) Measurement of extensional viscosity of polymer solutions. J Non-Newton Fluid Mech 40(3):271–280
Soulages J, Schweizer T, Venerus DC, Hostettler J, Mettler F, Kröger M, Öttinger HC (2008a) Lubricated optical rheometer for the study of two-dimensional complex flows of polymer melts. J Non-Newton Fluid Mech 150(1):43–55
Soulages J, Schweizer T, Venerus DC, Kröger M, Öttinger HC (2008b) Lubricated cross-slot flow of a low density polyethylene melt. J Non-Newton Fluid Mech 154(1):52–64
Taylor GI (1934) The formation of emulsions in definable fields of flow. Proc R Soc Lond A 146:501–523
Venerus DC, Zhu SH, Öttinger HC (1999) Stress and birefringence measurements during the uniaxial elongation of polystyrene melts. J Rheol 43(3):795–813
Wales JLS (1976) The application of flow birefringence to rheological studies of polymer melts. PhD thesis, Delft University of Technology, Delft
Verbeeten WMH (2001) Computational polymer melt rheology. PhD thesis, Technische Universiteit Eindhoven